REPORT DOCUMENTATION PAGE

AFRL-SR-BL-TR-01-

0234

88

1. AGENCY USE ONLY *(Leave blank)*	2. REPORT DATE	3. REPORT TYPE AND DATES COVERED
	20 Mar 01	Final Report: 01 Jun 96 TO 31 May 00

4. TITLE AND SUBTITLE

DEVELOPMENT AND MULTIPLEXING OF FIBER-OPTIC PRESSURE TRANSDUCERS

5. FUNDING NUMBERS

F49620-96-1-0227

6. AUTHOR(S)

DR. Kent A. Murphy

7. PERFORMING ORGANIZATION NAME(S) AND ADDRESS(ES)

The Bradley Department Of Electrical Engineering
340 Whittemore Hall
Virginia Tech
Blacksburg, VA 24061-0111

8. PERFORMING ORGANIZATION REPORT NUMBER

9. SPONSORING/MONITORING AGENCY NAME(S) AND ADDRESS(ES)

AFOSR/NA
801 N. Randolph St.
Arlington VA 22203

10. SPONSORING/MONITORING AGENCY REPORT NUMBER

11. SUPPLEMENTARY NOTES

12a. DISTRIBUTION AVAILABILITY STATEMENT

Approved for public release: Distribution is unlimited.

13. ABSTRACT *(Maximum 200 words)*

Conducted temperature and pressure tests of the silicon based temperature/pressure sensors, tested a micromachined, differential pressure sensor, characterized fiber optic sensor attachment and construction methods, fabricated and evaluated prototype high frequency signal processing system.

14. SUBJECT TERMS

Multiplexing, Fiber-Optic, Pressure Transducers

15. NUMBER OF PAGES

16. PRICE CODE

17. SECURITY CLASSIFICATION OF REPORT	18. SECURITY CLASSIFICATION OF THIS PAGE	19. SECURITY CLASSIFICATION OF ABSTRACT	20. LIMITATION OF ABSTRACT
UNCLASSIFIED	UNCLASSIFIED	UNCLASSIFIED	URL

Development and Multiplexing of Fiber-Optic Pressure Transducers

Dr. Kent A. Murphy, Principal Investigator

The Bradley Department of Electrical Engineering
340 Whittemore Hall
Virginia Tech
Blacksburg, VA 24061-0111

Contract: F49620-96-1-0227

Objectives

The objective of this research is to produce thermally stable multiplexed fiber-optic pressure transducers.

Status of Effort

The following has been performed during the reporting period:

- Conducted temperature and pressure tests of the silicon-based temperature/pressure sensors,
- Tested a micromachined, differential pressure sensor,
- Characterized fiber optic sensor attachment and construction methods,
- Fabricated and evaluated prototype high frequency signal processing system.

Accomplishments

Fiber-Optic Pressure Transducer Packaging

The sensing element of the fiber optic pressure sensor designed and developed by Luna Innovations was a micromachined structure fabricated by outside contractors. Shown in Figure 1, the sensing elements were mass produced with an ultrasonically machined Pyrex base wafer and a silicon wafer, which were anodically bonded together and diced into individual sensing elements. For each sensing element, the machined portion of the Pyrex base forms a cavity with the silicon wafer bonded to the surface. The portion of the silicon wafer that remains after dicing acts as a diaphragm and is designed to deform under pressure.

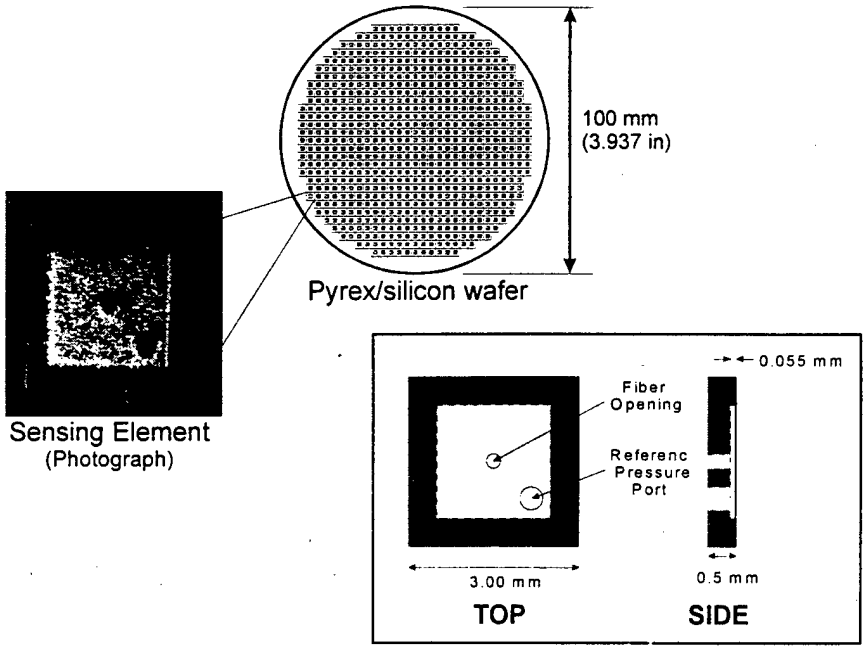

Figure 1. Micromachined sensing element for the fiber optic pressure sensor.

The size of the machined cavity, the diaphragm material properties and the diaphragm thickness are critical design criteria in determining the measurement range of the sensor. Designs for two sensing elements were developed for two sensors with linear ranges of 3 psi and 20 psi. The cavity dimensions were the only difference between the two designs, thus creating sensing elements with two different active sensing areas. Active areas were 4.0 mm^2 for the 3 psi design and 1.96 mm^2 for the 20 psi design.

The fully assembled sensor is shown in Figure 2. An optical fiber and hollow core fiber spacer are bonded in the center opening of the sensing element using epoxy. The gap between the bottom of the diaphragm and the end face of the fiber is a Fabry-Perot cavity. Using patented EFPI-based signal processing technology, light interference resulting from the internal reflection of light at the fiber end face (R_1) and reflected light off of the bottom surface of the diaphragm (R_2) is used to monitor the optical gap. The gap varies with diaphragm deflection, which in turn varies with applied pressure. The reference port on the bottom of the sensing element acts as a vent through which air can pass to maintain a constant pressure on the reference side of the diaphragm. Given a constant reference pressure, the diaphragm deflection can be directly related to changes in pressure on the measurement side. Representative room temperature performance characteristics for both sensor designs are shown in Figure 3. The large area sensor (4.00 mm^2 active area) is linear up to approximately 3 psi and the small area sensor (1.96 mm^2 active area) is linear up to 20 psi. Generally, sensitivities in the linear range of the large and small area sensors range between 0.5 to 0.7 psi/micron and 3 to 5 psi/micron, respectively.

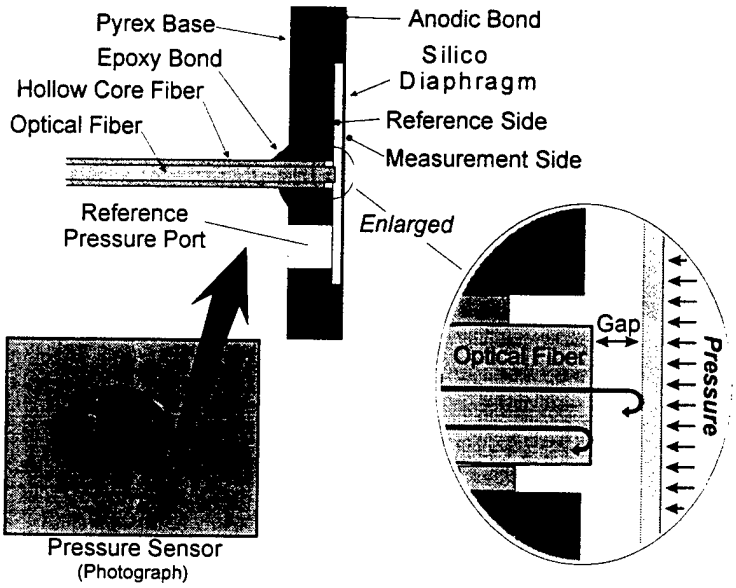

Figure 2. Assembled fiber optic pressure sensor.

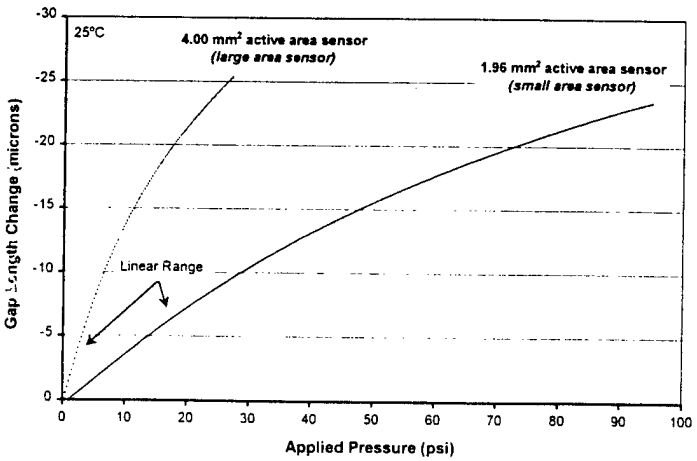

Figure 3. Representative pressure characteristics of fiber-optic pressure sensors.

Pressure Sensor Characterization

Characterization and optimization of the micromachined, fiber optic pressure sensor was a continuous effort during the program. The work focused on assessing the operating characteristics of the sensor as well as improving operability and fabrication procedures.

Repeatability

Non-repeatability of the pressure sensor design was determined by pressure cycling several of the sensors using a digital pressure controller. Several large and small area sensors were run through pressure cycles over a short period and at constant temperature. Figure 4 shows data from one such run, where a large area pressure sensor was cycled ten times at room temperature. For this particular sensor, non-repeatability is slightly less than ±1% of full scale, where full scale is defined as the linear range of the pressure sensor (0-3 psi). All ten of the generated pressure response curves in the figure tend to overlap, which provides a more visual confirmation of repeatability. The data shown in the figure are representative of test data collected during all the repeatability tests of this sensor design. For both the large and small area sensors, non-repeatability tends to be approximately ±1% FS at room temperature.

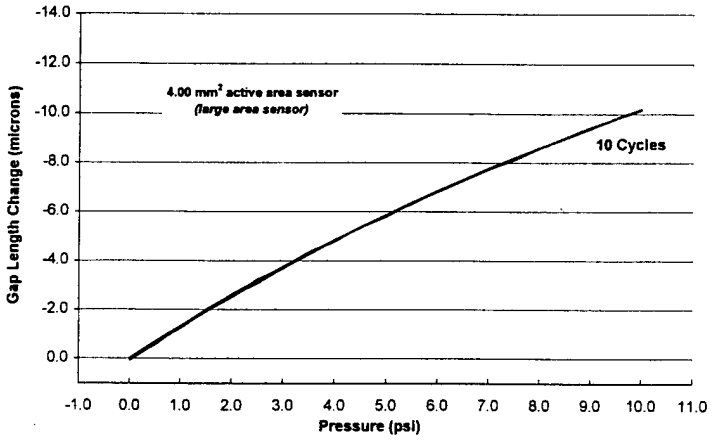

Figure 4. Example of pressure sensor repeatability data.

The data collected during repeatability testing also show that these sensors can withstand pressure several times their linear range without damage, allowing the sensors to be used well beyond their linear range if necessary. Although the sensor characteristics determined during this program are usually expressed as a percentage of linear range (defined as full scale), these pressure sensors are quite capable of operating normally beyond their linear range. The linear range is used only as a reference because it can be consistently determined.

Temperature Behavior

Some of the temperature characteristics of the pressure sensor design were determined using a dual temperature/pressure testing apparatus constructed for this purpose. It was anticipated that the sensor design would show at least some temperature sensitivity due to thermal expansion and temperature-related changes in the index of refraction of the air in the gap. To determine this sensitivity, several large and small area sensors were tested by running the sensors through several pressure cycles in much the same manner as the repeatability tests but at several different temperatures. The data shown in Figure 5 were acquired during one such series of tests. Starting at room temperature (25° C), this sensor was pressure cycled once at each of the temperatures shown up to 500° C. Visual analysis confirms that significant changes in sensitivity and zero offset occurred as the temperature was increased.

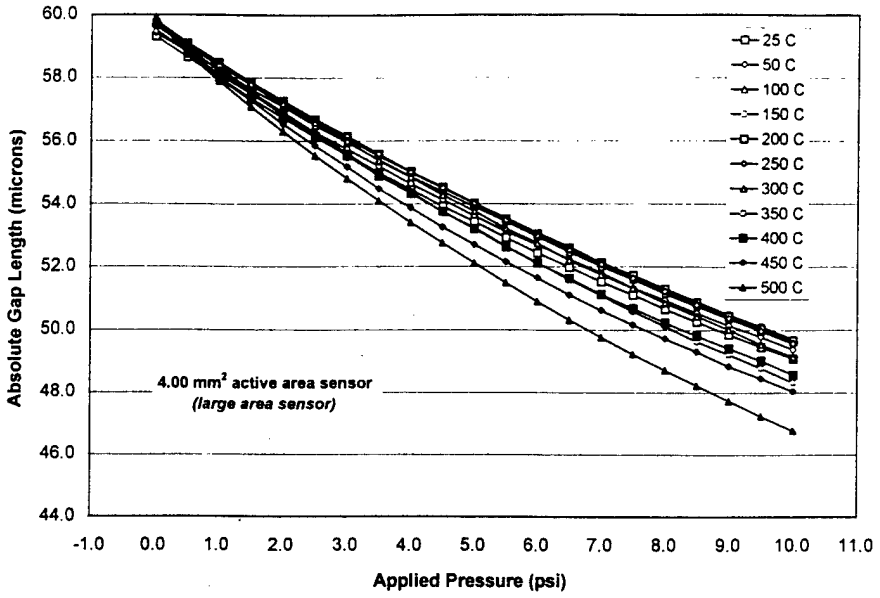

Figure 5. Temperature characterization data for a representative large area sensor.

Frequency Response

The frequency response characteristics of the fiber optic, micromachined, pressure sensor design were determined during a shock tube test at Wright State University (WSU). The WSU shock tube, shown in the photograph in Figure 6 (a), is a simple expendable diaphragm design that can be automatically triggered to coincide with high-speed data acquisition. A 20 psi range (1.96 mm^2 active area), fiber optic pressure sensor was installed in a fixture with a co-located high-frequency, piezoresistive pressure sensor. The fixture was mounted on the side wall of the WSU shock tube for testing, as shown in Figure 6 (b). Data from the fiber optic sensor were acquired using the dual wavelength system described later in the report. This system possessed adequate frequency response characteristics to resolve the high-frequency behavior of the fiber optic pressure sensor. Conventional high-speed signal processing equipment was used to acquire data from the piezoresistive pressure sensor. Data from the best test run in the shock tube are shown in Figure 7. Data from both sensors are smoothed (filtered) using a 10-point moving average to eliminate spurious signals. The data from both sensors show virtually the same response to a moving shock wave. The piezoresistive pressure sensor is known to possess a natural frequency greater than 200 kHz, so data from this sensor should show the general behavior shock wave. Since both sets of data tend to agree reasonably well, the high frequency capability of the fiber optic pressure sensor seems to be at least as good as the piezoresistive sensor. A power spectrum of the unfiltered fiber optic sensor data is shown in Figure 7 (b). The data show the resonant response of the fiber optic sensor, which occurred at approximately 137 kHz.

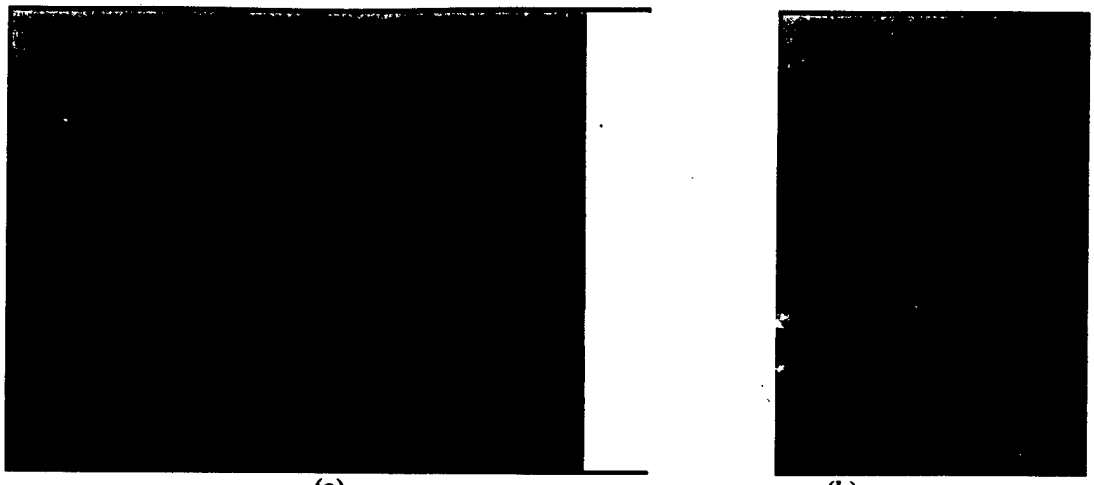

(a) (b)

Figure 6. WSU shock tube (a) and sensor fixture mounted in the shock tube (b).

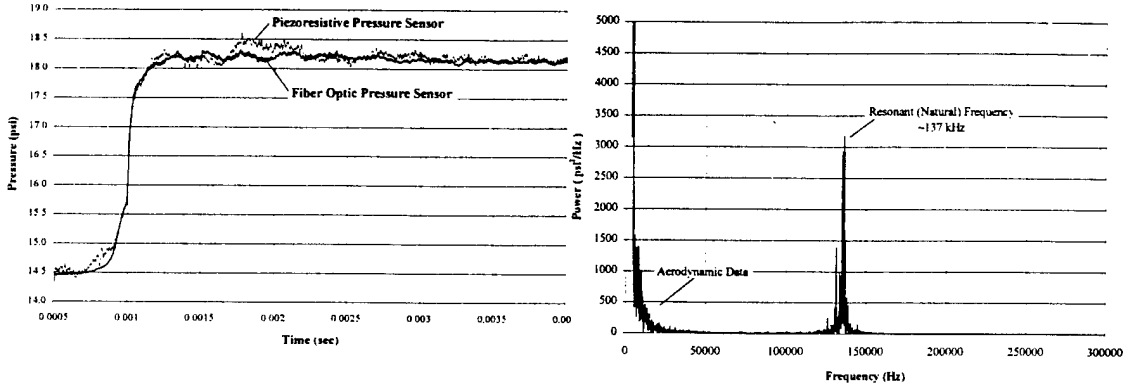

(a) (b)

Figure 7. Time history (a) and power spectrum (b) of fiber optic sensor data from WSU test.

Thermal Effects on Pressure Sensor Design

One problem with fiber optic pressure transducers is the effect of temperature on the pressure measurement. Several optical fiber, silicon-based, pressure sensors were tested to demonstrate and quantify this dependence. The thermal testing of the sensors demonstrated a significant thermal dependence in pressure measurement as shown in Figure 8. One method used to decrease the temperature effect is through the use materials with low coefficients of thermal expansion (CTE). One of the largest sources of temperature effects is due to the epoxy used to construct the sensors. To create a pressure sensor that will be repeatable at high temperatures, a replacement is needed for the epoxies that are currently used.

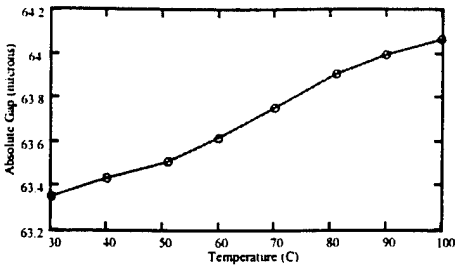

Figure 8. Thermal dependence of small diaphragm pressure sensor.

Two methods for eliminating the use of epoxies have been tried. The first one replaces the epoxy with solder glass. Solder glass is a low melting point glass with small quantities of lead and indium, to wet normal silica glass, and other fillers to change the CTE. Solder glass was originally created to hermetically seal CRT tubes. It is now used in a variety of products to seal pieces together. When using solder glass, considerable stresses may arise from any CTE mismatch. To minimize damage to parts and improve sealing, similar CTE's are necessary. Several samples of solder glass were obtained, however all had CTE's that matched silicon. Several attempts were made to attach a silica fiber to a silica tube, however, even with a very slow cool down rate, the parts still shattered due to the difference in CTE. Problems also occurred with adhesion of the silica tube to the fiber. Solder glass is intended to be sandwiched between silica parts, but because of the diameter of the tube, this was not a possibility. When the solder glass was placed on the part, no wetting occurred; the solder glass flaked off.

The second way tried to eliminate epoxy was fusion splicing. Fusion splicing attempts to melt the glass hollow core tube onto the fiber. Both tube and fiber are first stripped of polyimide and cleaned and aligned in the fusion splicer. The heating element then is ramped to a high enough temperature to partially melt the tube onto the fiber. While this method works well in the creation of normal strain gage EFPIs, it does not work for fusing silica fiber to silicon.

One way to thermally compensate pressure transducers utilizes a refractive index change of the diaphragm to detect temperature. In an EFPI-type fiber-optic pressure transducer, three interferomic signals are returned to the fiber from the diaphragm (Figure 9). The first signal is caused by the interference of a reflection from the end of the fiber (R1) and a reflection from the near side of the diaphragm (R2). The second signal is caused by the interference of a reflection from the near side of the diaphragm (R2) with the light that travels through the diaphragm and reflects off the far side of the diaphragm (R3). The third signal is caused by the interference of a reflection from the end of the fiber (R1) and a reflection from the far side of the diaphragm (R3).

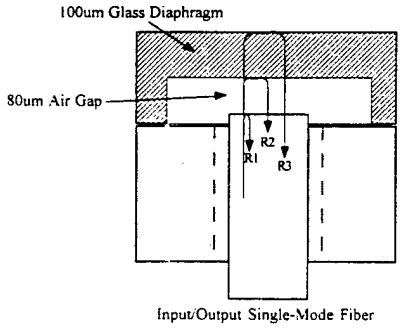

Figure 9 Typical fiber optic pressure transducer design.

A pressure transducer was constructed with an air gap of around 80μm and a diaphragm thickness of 100μm. This transducer was connected to a source/detector box interfaced with a laptop computer. The returned wave spectrum and demodulated spectrum can be seen in Figure 10.

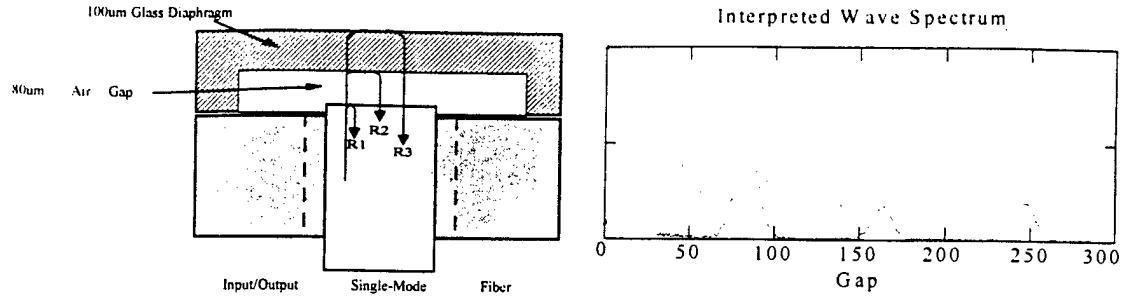

Figure 10. a) Returned wave spectrum from the pressure transducer. b) Demodulated spectrum showing the three signals detected: the air gap, the glass thickness, and the combination of the two.

The tip of each of the sensor peaks is the measured gap length of each sensor. The first peak, at around 80μm, tracks the air gap between the fiber and the diaphragm. The second peak, at around 160μm, tracks the thickness of the glass diaphragm. The demodulation system is designed to measure air gaps. Because the second peak is measuring the thickness of glass and not air, one must divide by 1.5 (the approximate index of refraction of glass) to get the actual thickness of the glass diaphragm. After this adjustment, the thickness of the diaphragm is measured around 100μm, which matches the actual thickness. The third peak at around 240μm tracks the air gap plus the thickness of the glass. To verify this interpretation of the three signals theoretically, the measured value of the third peak was compared to the summation of the first two peaks. The third peak measurement was within 0.05% of the summation of the first two peaks.

In measuring the glass thickness over a temperature range, the value will vary due to the refractive index change of the glass; the actual change in the thickness of the glass will be negligible. By dividing the measured glass thickness by the actual glass thickness, the change in index of refraction with changing temperature can be tracked. By measuring the change in index of refraction of glass to measure temperature, the pressure transducers can be thermally compensated. This method of thermal compensation has several advantages. The main advantage is that it does not require any additional sensors to measure temperature. A secondary advantage is that it measures temperature at the same location it measures pressure.

Serially Multiplexed Fiber-Optic Pressure Transducers

One approach to multiplexed fiber-optic sensors uses Gap Division Multiplexing (GDM). In this approach a broadband laser diode source is used to interrogate sensors biased at different gap lengths and limited to certain gap ranges. These sensors can be either serially multiplexed (all in the same fiber) or spatially multiplexed (using a star coupler). A limitation of gap division multiplexing is the inability to demodulate sensors operating at gap ranges that are integral multiples of one another (e.g., one at 50μm and another at 100μm). This is due to the nature of the mathematical computations involved in demodulating the spectrum. This limitation requires that a buffer region separate the sensor bias points, preventing interference between the signals. It was found previously that the minimal buffer region should be 30μm.

Four multiplexed EFPI sensors were successfully demonstrated with one fiber optic measurement system. The four sensors consisted of two channels with two serially multiplexed sensors on each channel. The sensors had gaps of 30, 90, 150, and 210 microns. They were biased such that the signals from combinations of the sensor signals would not interfere. The 30 micron and 90 micron signals combine to form an additional signal at 120 microns, which minimizes the interference between the neighboring

signals due to the fact the nearest sensor signals are still 30 microns away. The returned spectrum from the four multiplexed sensors is shown in Figure 11. The individual sensor signals, after demodulation, are shown in Figure 12.

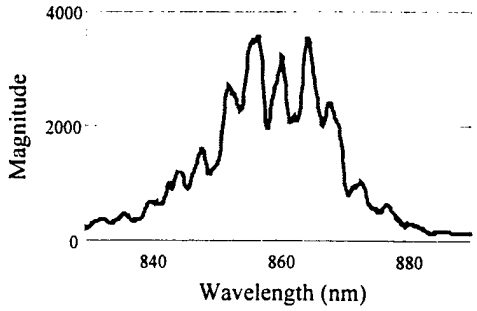

Figure 11. Spectrum for four multiplexed EFPI strain sensors

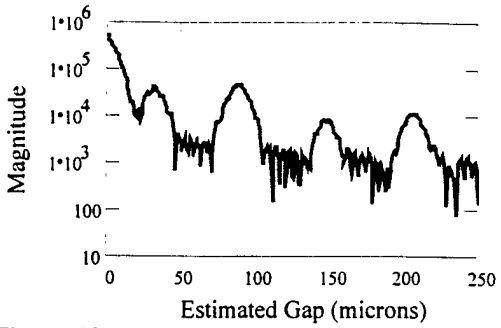

Figure 12. Power spectral density plot showing the four EFPI signal peaks

Future work in this area will consist of testing the multiplexed sensors by independently changing the strain or the pressure on the individual sensors, and testing to evaluate cross talk between serially multiplexed sensors.

High Frequency Measurement System

The transducing mechanism used by these sensors is based on the extrinsic Fabry-Perot interferometer (EFPI) developed by Kent Murphy et al. EFPI-based sensors use a distance measurement technique based on the formation of a low-finesse Fabry-Perot cavity between the polished end face of a fiber and a reflective surface, shown schematically in Figure 13. Light is passed through the fiber, where a portion of the light is reflected off the fiber/air interface (R1). The remaining light propagates through the air gap between the fiber and the reflective surface and is reflected back into the fiber (R2). These two light waves interfere constructively or destructively based on the path length difference traversed by each. In other words, the interaction between the two light waves in the Fabry-Perot cavity is modulated by the path length. The resulting light signal then travels back through the fiber to a detector where the signal is demodulated to produce a distance measurement. Several different demodulation methods exist to convert the return signal into a distance measurement.

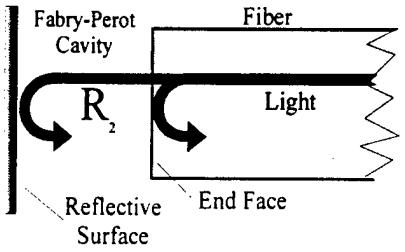

Figure 13. Extrinsic Fabry-Perot Interferometer Concept

Demodulation using single wavelength interrogation

A basic demodulation system using single wavelength interrogation is shown in Figure 14.

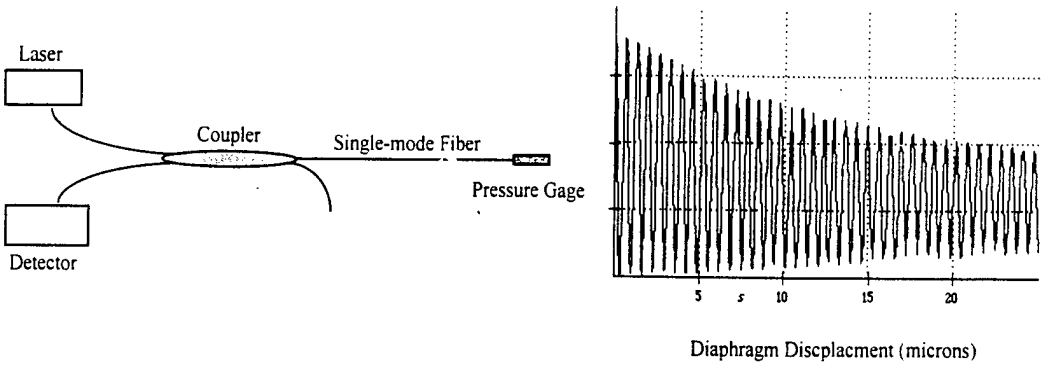

Figure 14. Basic Demodulation System and Typical Output of EFPI Pressure Sensor

A laser diode supplies coherent light to the sensor head and the reflected light is detected at the second leg of the optical fiber coupler. The output can then be approximated as a low-finesse Fabry-Perot cavity in which the intensity at the detector is,

$$I_r = |A_1 + A_2|^2 = A_1^2 + A_2^2 + 2A_1A_2\cos\Delta\phi\,, \qquad (1)$$

if A_1 and A_2 are the amplitudes of R1 and R2, and $\Delta\phi$ is the phase difference between them. The output is then a sinusoid with a peak to peak amplitude and offset that depends on the relative intensities of A_1 and A_2. A phase change of 360 degrees in the sensing reflection corresponds to one fringe period. If a source wavelength of 1.3 μm is used, the change in gap for one fringe period is 0.65 μm. The drop in detector intensity is due to the decrease in coupled power from the sensing reflection as it travels farther away from the single-mode input/output fiber. By tracking the output signal, minute displacements are determined. The disadvantage of this type of demodulation system is the non-linear transfer function and directional ambiguity of the sinusoidal output.

An approach to solving these problems is to design the sensor head so that at the maximum gap the signal does not exceed the linear region of the transfer function. Confining the operation to the linear region places difficult manufacturing constraints on the sensor head by requiring the initial gap to be positioned at the Q-point of the transfer function curve. In addition to the difficult manufacturing constraints, the resolution and accuracy are limited when the signal output is confined to the linear region. If acceleration changes occur at a peak or valley in the sinusoid as shown in Figure 15 at π, 2π, 3π, ..., they will not be detected because the slope of the transfer function is zero at those points. The sensitivity of the system correspondingly decreases at points near multiples of π. If the direction of diaphragm movement changes at a peak or valley, that information is lost, which causes directional ambiguity in the signal.

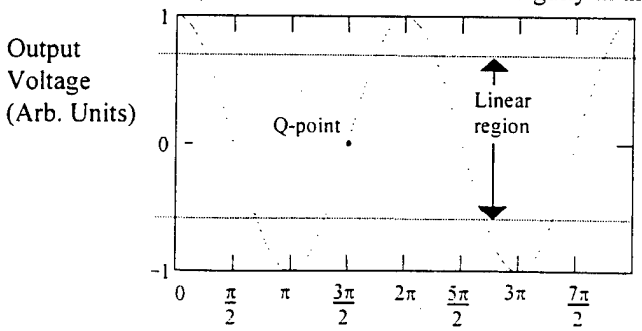

Figure 15. Interferometric signal output.

One approach to solving the aforementioned problems is to design the sensor head so that at maximum acceleration, the signal does not exceed the linear region of the transfer function. The linear region of the sinusoidal transfer function is shown in Figure 15. Confining operation to the linear region places difficult manufacturing constraints on the sensor head by requiring the initial gap to be positioned at the Q-point of the transfer function curve. In addition to the difficult manufacturing constraints, the resolution and accuracy are limited when the signal output is confined to the linear region.

Dual Wavelength Approach

One approach which solves the non-linear transfer function and directional ambiguity problems is to use a dual wavelength interrogation system. By properly choosing the wavelengths, outputs which are ninety degrees out of phase, or in quadrature, can be obtained. Figure 16 shows a theoretical plot of the reflected intensities that can be obtained with this system. As seen from the graph, when one signal is at a peak or valley, the other signal is in the linear region. In this way, one signal always has a linear response with acceleration. By monitoring the phase lead/lag relationship between the signals, the direction of diaphragm movement is unambiguously determined. An output showing the phase lead/lag relationship at a direction change, or turnaround, is shown in Figure 17.

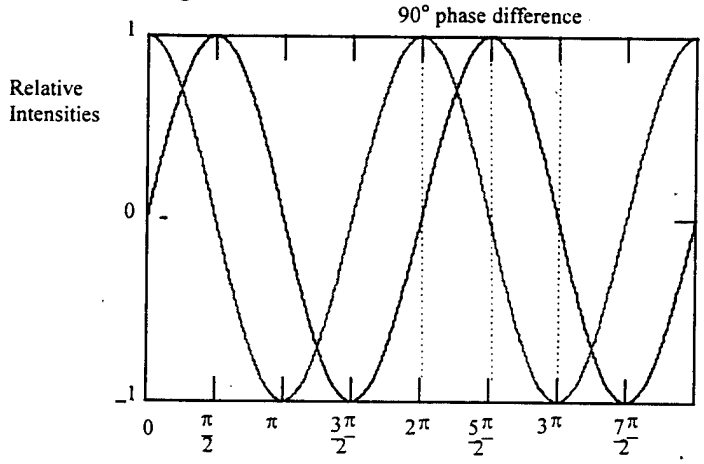

Figure 16. Theoretical outputs of quadrature signals obtained from a dual wavelength system.

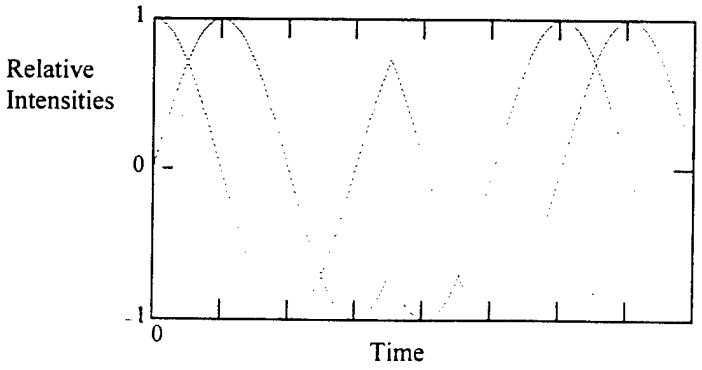

Figure 17. Two wavelength system theoretical output showing the phase lead/lag relationship at a direction change.

Demodulating Quadrature Signals

Figure 18 shows a simulated sinusoidal disturbance to an EFPI sensor. Figure 19 shows the corresponding response of both of the quadrature signals as would be received by a photodetector.

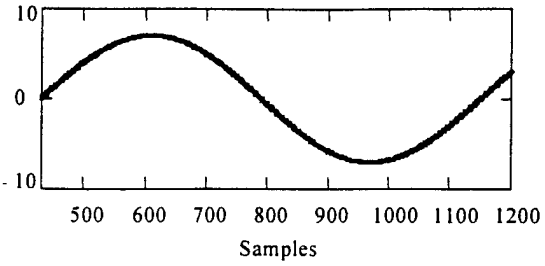

Figure 18. Sinusoidal perturbation of the EFPI sensor.

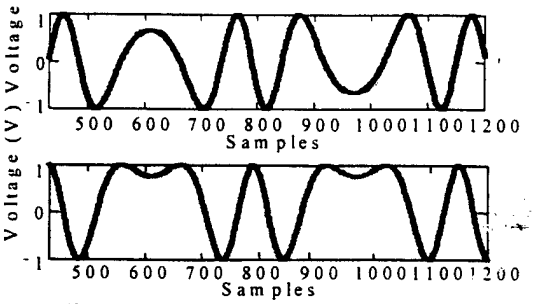

Figure 19. Quadratic response from two wavelengths.

As the quadratic perturbation drives the EFPI sensor through a fringe, the Lissajous plot traces a revolution on the circle in Figure 20. One revolution around the circle is the equivalent to going through one fringe (630nm), and by tracking the perturbation around the circle one can track the change in gap. The perturbation is tracked around the circle by monitoring the change in α, which is given by the arctangent of V1/V2.

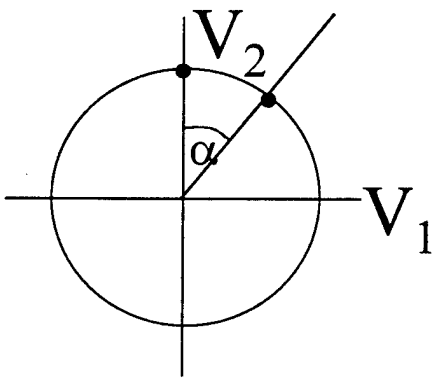

$$\alpha = \tan^{-1}(V_1/V_2)$$

Figure 20. Lissajous plot from the two wavelengths

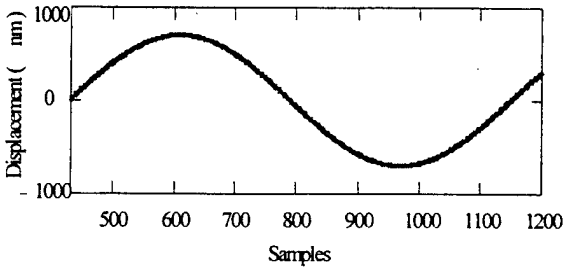

Figure 21. Sinusoidal perturbation as measured by two-wavelength measurement system.

By tracking the rotations around the circle and converting α to a displacement value the perturbation in terms of gap change can be found (Figure 21). In the finished system this displacement can then be converted into a voltage proportional to the measured strain or pressure – depending upon the sensor used.

Building the Dual Wavelength Demodulation System

A candidate dual wavelength architecture is shown in Figure 22. The design utilizes two quadrature optic channels and digital signal processor to provide unambiguous, accurate, high frequency measurements. Two lasers of appropriate output wavelength are selected to generate quadrature phase shifted signals for a given sensor air gap. The reflected laser signals from the sensor head are then separated out at the detector end using optical filters. The quadrature signals are sent to the digital signal processor for high-speed demodulation into an output analog signal that corresponds to the relative movement of the interferometric cavity.

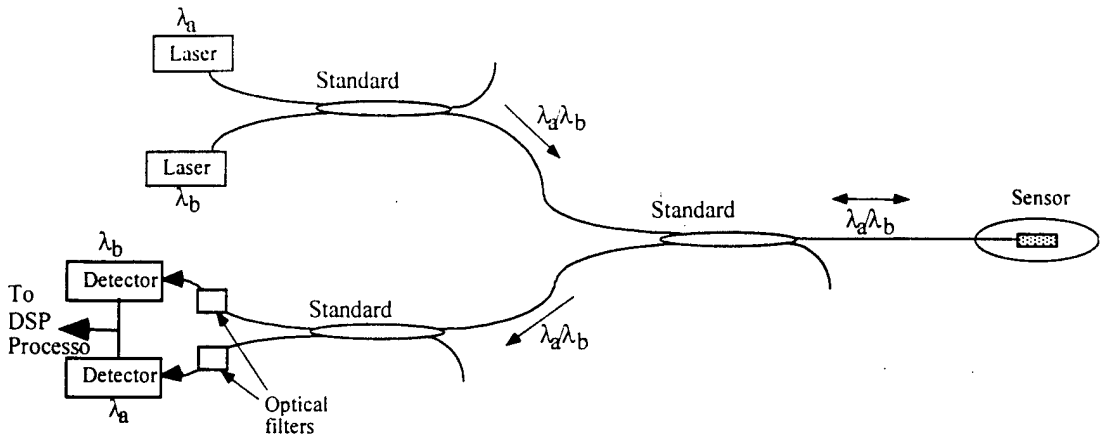

Figure 22. Dual wavelength interrogation system for accelerometer.

A prototype of the above system was created in order to show the feasibility of a dual wavelength demodulation system and is shown in Figure 23. This system was tested with a fiber optic accelerometer to generate dynamic sensor conditions necessary to verify the system operation. The results of the dynamic testing are shown in Figure 24 and Figure 25. The scope trace shown in Figure 24 shows the quadrature signals in almost perfect alignment – as seen by the roundness of the circle – operating at a frequency of 250 Hz. The trace in Figure 25 shows the same two quadrature signals, the output of the dual wavelength system, and the output of a reference, conventional accelerometer. Notice the strong agreement between the output of the fiber optic system and the calibration system.

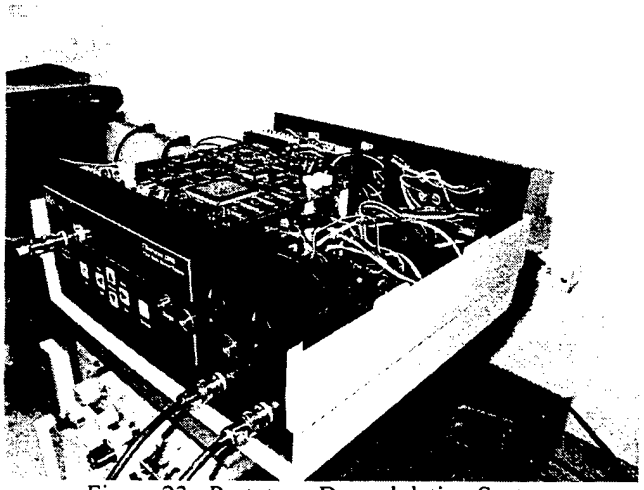

Figure 23 . Prototype Demodulation System

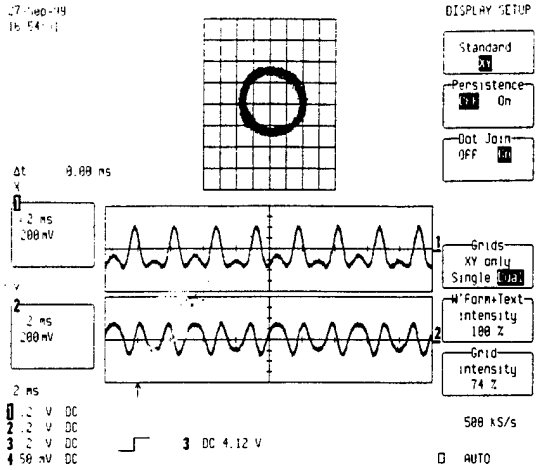

Figure 24. Lissajous Plot

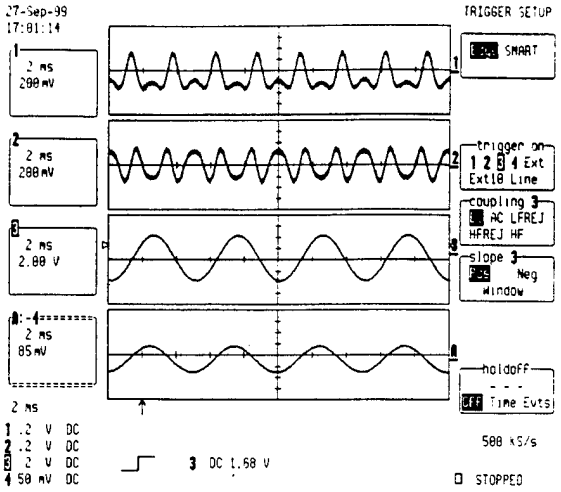

Figure 25. Demodulation Output Signals

The main limitation of the dual wavelength system is that it requires a calibration procedure whenever the optical channel in the system is reconfigured. This is due to the fact that the system operation is based on the returned intensity of the two wavelengths. This requires a repetitive perturbation of the system through several cycles in order to adjust the gain and offset of the demodulation circuitry. In order to alleviate this requirement, F&S researchers have designed self-modulating capabilities into the sensors to be used with the dual wavelength system. The new design will allow physical perturbation of the mass by using electro-static forces transmitted through two conductors contained in the cable assembly. However, the electrical channels are used only during initial calibration and remain shunted during normal operation.

Personnel

Jason Dietz, Jason Borinski, Tom Wavering, Pat Russler, and Alex Edwards.

Publications

"NDE Characterization of Advanced Composite Materials with High Temperature Optical Fiber Sensors," T. Wavering, et. al., SPIE Symposium on Smart Structures and Materials, March 1999.
"NDE Characterization of Composites with High Temperature Optical Fiber Sensors ", T. Wavering, et. al., SAMPE, Long Beach, CA, May 1999.
"Developments in fiber optic sensor technology for harsh environments," 45th International Instrumentation Symposium, 1999

Interactions/Transitions

SPIE Symposium on Smart Structures and Materials, March 1999.
SAMPE, Long Beach, CA, May 1999
ASME Gas Turbine and Aeroengine Technical Congress, 1999
AIAA Joint Propulsion Conference, 1999
International Instrumentation Symposium [IIS], 1999

The fiber optic pressure sensor, thermal compensation, materials, and high frequency demodulation development and research under this program is currently benefiting the following programs:

USAF, WPAFB, Developing high temperature optical fiber strain and pressure gages.
USAF, WPAFB, Developing optical fiber skin friction and pressure gages for wind tunnel applications.
Advanced Processing Technologies, Developing multiplexed optical fiber strain and pressure gages.

Northrop, Developing multiplexed optical fiber strain and pressure gages for the Smart Wing program
USAF, AEDC, Developing high temperature strain sensors.
NASA, Dryden, Developing optical fiber accelerometers for in-flight applications.
NASA, Langley, Developing optical fiber skin friction gages for wind tunnel testing.

Discoveries, Inventions, and Patents

None this reporting period.

Honors/Awards

None this reporting period.

February 26, 2001

AFOSR/PKA
ATTN: Brian P. Saunders, Major, USAF
801 North Randolph Street, Room 732
Arlington, VA 22203-1977

RE: Contract: F49620-96-1-0227

Dear Major Saunders:

Enclosed are two (2) originals of the final report for the referenced contract.

I appreciate you support of this research effort.

Sincerely,

Kent A. Murphy

Kent A. Murphy, Ph.D.

Enclosure